Effect of Gold Substrates on the Raman Spectra of Graphene

Nayoung Kim,[†] Min Kyung Oh,[†] Sungho Park,[†,‡,§] Seong Kyu Kim,[†,*] and Byung Hee Hong[†,‡,#]

[†]*Department of Chemistry,* [‡]*SKKU Advanced Institute of Nanotechnology (SAINT),* [§]*Department of Energy Science,
and* [#]*Center for Human Interface Nano Technology (HINT),
Sungkyunkwan University, Suwon 440-746, Korea.* [*]*E-mail: skkim@skku.edu*

Raman spectra of a single layer graphene sheet placed in different gold substrates were obtained and are discussed in the context of surface enhanced Raman scattering (SERS). The gold substrates were composed of a combination of a thermally deposited gold film and a close-packed gold nanosphere layer. The SERS effects were negligible when the excitation wavelength was 514 nm, while the Raman signals were enhanced 3- to 50-fold when the excitation wavelength was 633 nm. The large SERS enhancement accompanied a spectral distortion with appearance of several unidentifiable peaks, as well as enhancement of a broadened D peak. These phenomena are interpreted as the local field enhancement in the nanostructure of the gold substrates. The difference in the enhancement factors among the various gold substrates is explained with a model in which the spatial distribution and polarization of the local field and the orientation of the inserted graphene sheet are considered important.

Key Words: Graphene, Raman, Gold, Nanoparticles, Surface Enhanced Raman Scattering

Introduction

Since micromechanical cleavage of graphite crystals provided the first isolated graphene in 2004,[1] graphene has been one of the most intensively studied materials for the past few years owing to its unique physical properties and potential applications. The methods of preparing a monolayer or a few layers of graphene in large sizes or in defect-free states are under current development.[2-4]

One of the most popular nondestructive methods to analyze for synthesized graphene is Raman spectroscopy. Due to the unique electronic band structure,[5,6] the Raman scattering of graphene is a resonance process sensitive to the degree of disorder and the number of layers. In the graphene Raman spectra in visible wavelengths, three characteristic peaks have been well studied.[7-13] The peak near 1580 cm^{-1}, or the G band, is assigned to an in-plane asymmetric translational motion of two nearby carbon atoms (E_{2g} mode). This is a degenerated optical phonon mode at the Brillouin zone center (the Γ point of the reciprocal lattice space), and is induced by a single resonance process. The peak near $1300 \sim 1400$ cm^{-1} is denoted with the D band, an in-plane carbon ring breathing mode (A_{1g} mode), forbidden in perfect graphite. The peak position of the D band is dependent on the excitation wavelength, which is explained by a double resonance process at the K point of the reciprocal lattice space. This process requires a scattering at defect sites in order to conserve the momentum. For this reason, the D band has been considered a measure of disorder in graphite crystals and has been found dominant at the edge sites of a single layer graphene.[11] The double resonance process also induces an activation of two phonons, whose peak appears between $2600 \sim 2800$ cm^{-1}. Since this peak frequency is close to double the frequency of the D band, it is denoted with the 2D, while other authors refer to it with the old-fashioned G' band. The resonance process for the 2D band is momentum-conserved and does not require the scattering at defect

sites. The 2D peak position is sensitive to the excitation wavelength and the graphene layer, and therefore its band shape can be used to identify the number of graphene layers.[3,4,12,13]

When graphene is placed on a substrate, the substrate-graphene interaction may modify the band structure. In the case of weak interactions with substrates such glass, sapphire and ITO, the graphene Raman spectra show slight peak shifts.[14-19] In this report, a case of a metal substrate was investigated with a view to study metal-graphene hybrid structures. Substrates made of gold were chosen and discussed in the context of surface enhanced Raman scattering (SERS). In general, two mechanisms are considered to be important in the SERS phenomena.[20] The first is a chemical mechanism (CM) where a new resonance state is generated through a charge transfer between the substrate and adsorbate. The second is an electromagnetic mechanism (EM) in which a local electric field is greatly enhanced in certain noble metal nanostructures, such as sharp shapes or gaps (so-called "hot spots").

Since the graphene is in the form of a 2-dimensional sheet, the metal substrate in the form of a 2-dimensional film is first considered. In a flat gold film, one may expect a charge transfer between graphene-gold and an enhancement of Raman peaks through the CM. In contrast, the EM is expected to be relatively small because of lack of hot spots. The EM can be activated when noble metal nanoparticles are placed on the flat gold film. In this case, the enhanced local field is generated at the contact areas of the two structures by coupling the localized surface plasmon of the nanoparticles with the surface plasmon polariton of the flat film.[21-24]

Another variety of 2-dimensional structure is a close-packed nanoparticle layer, which can be obtained by compressing nanoparticles, after collected at the water-nonpolar liquid interface, with Langmuir-Blodget type barriers. The substrates produced in this way have proven effective SERS substrates,[25-28] as a high density of enhanced local electric field is generated at the contact

points between the nanoparticles. Interestingly, the SERS intensity increased as the number of closed-packed nanoparticle layers increased, which has been interpreted as an effective interlayer plasmon coupling, in addition to the intralayer plasmon coupling.[28,29]

Experimental Section

Graphene sheets were synthesized on thin Ni layers using a thermal chemical vapor deposition method with methane as a precursor.[2] From analyses with an optical microscope and Raman mapping, about 70% of the area in each graphene sheet was confirmed covered in a single layer (See Supporting Information). The synthesized graphene sheet was then transferred onto a substrate for the Raman study. Five different samples were prepared: (1) a graphene sheet transferred onto a 300 nm thick SiO_2 layer formed on a silicon wafer, (hereafter g-SI): (2) a graphene sheet transferred onto a 20 nm thick gold film deposited by thermal evaporation onto a silicon wafer, (hereafter g-Film): (3) a graphene sheet transferred onto a layer of close-packed gold nanospheres (NS) deposited onto a silicon wafer, (hereafter g-NS): (4) a layer of closed-packed gold nanospheres deposited onto the g-Film, (hereafter NS-g-Film): (5) a layer of close-packed gold nanospheres deposited onto the g-NS, (hereafter NS-g-NS).

Preparing a layer of closed-packed gold NS followed a previously described method.[25-28] Briefly, gold spheres (13 nm diameter) were first synthesized in water by reducing $HAuCl_4 \cdot 3H_2O$ with trisodium citrate. Then, by adding hexane and ethanol, the gold NS were collected to form a coarse monolayer film on the water surface. Compressing the film with Langmuir-Blodget type barriers produced a monolayer of close-packed gold NS. The compressed monolayer film can be transferred onto a solid substrate without distortion of the close-packing structure. The transfer process can be repeated if a multilayer film is to be obtained. The extinction spectra of this kind of films, reported previously,[25-28] show that a broad Plasmon band sets on *ca*. 500 nm and extends to near IR region.

The Raman spectra in this report were obtained using a micro-Raman spectrometer (Renishaw, InVia). The excitation laser beam at a wavelength of either 514 nm or 633 nm was focused by a 50× objective lens with a numerical aperture value of 0.75 onto about a 1 μm^2 area of the sample. The laser power at the focused spot was measured to be 2.6 mW for 514 nm or 4.7 mW for 633 nm. The scattered light was collected by the same objective lens and passed through a notch filter before being introduced into a monochromator with a Peltier-cooled CCD detector. Each Raman spectrum was obtained with a 10 s detector exposure time.

Three graphene sheets, produced under the same conditions, were used. The first was used for the g-SI, the second for the g-Film and NS-g-Film, and the third for the g-NS and NS-g-NS. In all the samples, the shapes of Raman spectra were consistent from laser-focused spot to spot unless the laser hit the edges or multilayer regions of the graphene sheet. Using a marker in the microscope, the Raman spectra were obtained from the same single layer spot of a given graphene sheet (e.g. the same spot for g-Film and NS-g-Film).

Results

Figure 1 shows the Raman spectra of single layer graphene sheets in a series of the five different substrates. The peak intensities of the gold-free graphene (g-SI) when the excitation was 514 nm were larger by about 20% than those when the excitation was 633 nm, although the laser intensity of the 633 nm excitation was higher by 73%. The G band at 1583 cm^{-1} and the 2D band at 2709 cm^{-1} (for the 514 nm excitation) or at 2683 cm^{-1} (for the 633 nm excitation) were observed as the major peaks. The intensity of the 2D band was approximately twice that of the G band for both excitation wavelengths; this trend persisted in all Raman spectra except the 633 nm case of the NS-g-NS sample. This implies that the Raman spectra were obtained from the single layer regions of the graphene sheets.[3,4]

The peak intensities of the g-Film were reduced from those of the g-SI when the excitation was at 514 nm, but increased several times at 633 nm. When the substrate contained layers of close-packed gold nanospheres, as in the g-NS, NS-g-Film, NS-g-NS samples, the spectral shapes changed significantly. The most apparent change was the formation of a broad background feature that appeared to grow from the short wavelength and decay to the long wavelength, which can be characterized as an emission band. The spectral change over the sample series was more apparent for the 633 nm excitation than the 514 nm excitation; the D band grew with increased bandwidth and several small unidentifiable peaks appeared in the g-NS, NS-g-Film, and NS-g-NS samples.

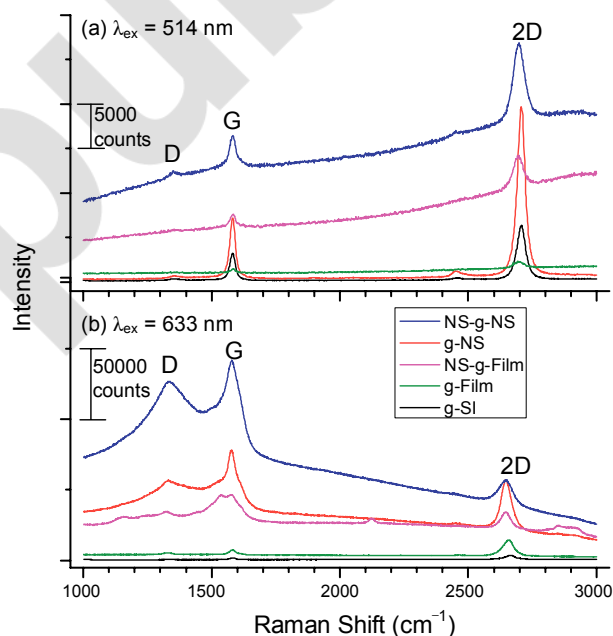During the acquisition of the spectra in Figure 1, there was a

Figure 1. Raman spectra of a graphene sheet in five different substrates. (a) and (b) are the cases for the two excitation wavelengths. All spectra are displayed without any data manipulation, such as background subtraction or intensity attenuation. The sample identity of each spectrum is indicated in the inserted window. Note that the order of the samples in the inserted window is the same as the order of background plateaus in the spectral series.

Table 1. Enhancement of the G band and 2D band from those of g-SI. The data marked # have larger uncertainties from the fit process, as much as 20%, while other data typically possess uncertainties of a few percent.

	G band		2D band	
	514 nm	633 nm	514 nm	633 nm
g-Film	0.13	3.2	0.11	11
NS-g-Film	0.48	#6.1	0.60	11
g-NS	2.2	#32	3.2	14
NS-g-NS	1.3	#50	1.5	15

concern regarding the damage of the graphene by the focused excitation laser. In one test, the dependency of the spectral shape upon the laser power was investigated. In all cases of the 514 nm excitation and the cases of the gold-free graphene sheets, the peak intensities varied linearly with laser power, while under the 633 nm excitation, the dependency in the gold-substrate samples was not linear. In another test, a spectrum was obtained with 10% of the full laser power, followed by illumination with the full laser power for 1 minute. Then, the spectrum was obtained again with 10% laser power. (The results of this test are shown in Supporting Information.) The intensities of the second spectrum were negligible within the experimental error for the 514 nm excitation or the gold-free graphene sheets, but were reduced by 10 ~ 30% for 633 nm excitation of the gold-substrate samples.

While some spectra induced by 633 nm excitations may be distorted slightly due to high laser power, an attempt to isolate Raman bands from the emission band was made; the broad background feature was subtracted out from each spectral data using a spline fitting. In some cases (the g-NS, NS-g-Film, and NS-g-NS samples in the 633 nm excitation), a deconvolution using a sum of lorentzian functions was necessary to isolate the peaks. The isolated peaks were then integrated and compared to different samples. In Table 1, the ratios of the integrated peak (G and 2D) intensities of the four gold-substrate samples to that of the g-SI are listed. The ratios correspond to the SERS enhancement factors. Although the ratios contain errors coming from the fit uncertainties and the laser-induced distortions, the following qualitative conclusions can be drawn: (1) the SERS enhancements at 514 nm excitation are not significant, while those at 633 nm excitation are appreciable; (2) the SERS enhancements are more significant in the g-NS and NS-g-NS than in the g-Film.

Discussion

When a graphene sheet is laid on a substrate of varied thickness, its Raman scattering may be modulated by an interference effect. A Raman enhancement as much as 30 can be induced when a dielectric layer is placed in between a graphene sheet and a reflecting substrate.[30] However, the Raman enhancement observed in this work cannot be attributed to such interference phenomenon, since there is no dielectric layer underneath the graphene sheet. Therefore, the observed Raman enhancements are interpreted in terms of the usual SERS mechanism.

When graphene is in contact with gold, it loses electron density as its Fermi level is shifted up nearly 0.2 eV.[31,32] The gra-

phene-gold bond is covalent in nature and has a weak interaction energy of approximately 0.04 ~ 0.1 eV per carbon atom.[32,33] This nature of the bonding works against the possibility of the CM for the observed SERS enhancement.

In the Raman spectra shown in Figure 1, the broad emission-like background appeared in the g-NS, NS-g-Film, and NS-g-N. The background cannot be attributed to an emission from a graphene-gold charge transfer state since it did not appear in the g-Film. In addition, in a separate experiment with a fluorescence spectrometer, similar emission bands from any of the samples were undetected. The emission-like background must result from a cooperation of the graphene, the gold NS, and the laser irradiation. Therefore, it would be reasonable to explain the SERS enhancement shown in the present data in terms of the EM.

The SERS enhancements shown in our data are not as large as those 10^6 which many molecular adsorbates on noble metal SERS substrates have demonstrated, but still have appreciable values of a few tens. Since the Raman process of graphene is a resonance process for itself, a newly formed charge-transfer state, if any, may not necessarily induce an additional enhancement to the resonance effect. On the other hand, the additional enhancement might be expected if the graphene is positioned properly in the nanostructure of the gold substrates to experience enhanced local field. Especially, the fact that the Raman enhancements were found much more significant at 633 nm than 514 nm leads us to explain the observed Raman enhancements in terms of the EM. (The extinction of the closed-packed gold nanosphere layer is an order of magnitude higher at 633 nm than 514 nm. Therefore, the SERS is more active at the 633 nm excitation than the 514 nm excitation.[25,29])

Since the thermally deposited gold film is more or less flat, the g-Film does not possess a high density of hot spots and therefore the SERS enhancement is expected to be small. For the g-Film, the enhancement factors were between 3 ~ 10, when the excitation was at 633 nm. This much enhancement may be induced by electric field localized in roughened parts of the gold film. In contrast, a close-packed gold NS layer has a high density of hot spots at the interparticle contact points; therefore, the g-NS, NS-g-Film, and NS-g-NS can be more SERS-active.

Further analysis of our results necessitates greater detailed information on the local field distribution. Recently, we have performed the local field calculation on layer-by-layer close-packed assemblies of gold nanospheres and nanorods using a finite difference time domain method.[29] (An example of the calculated local field distribution is shown in the Supporting Information.) From the calculated 3-dimensional mapping of the local field, a model in Figure 2 is presented.

In this model, the hot spots in the g-NS sample are generated primarily at the interparticle contact points (hot spot A). The maximum intensity of the hot spot is as much as $10^3 ~ 10^4$ and its intensity decreases rapidly upon going away from the spot center. The electric field of the hot spot is polarized along the interparticle coupling direction, or in the xy plane. (See Figure 2 for the definition of the axes.) If a graphene sheet lies flat on this substrate, it cannot experience the high local field from the hot spots, and the SERS enhancement would not be much greater than for the g-Film. However, a graphene sheet may
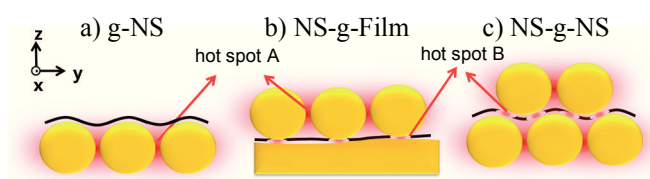
Figure 2. The model of the three SERS-active structures. In each structure, the red colored gradient depicts the distribution of the local electric field. The black sold curve represents the graphene sheet. The xyz coordinate is presented on the top left side.

corrugate to follow the curvature of a substrate, as is reported for a SiO_2 substrate.[34] Such a corrugation is also plausible for gold substrates since the interaction induces a rather large graphene distortion.[33] As parts of the graphene sheet approach the hot spots, a SERS enhancement much larger than the g-Film can be induced.

In the case of the NS-g-Film, a strong local electric field can be produced at the interlayer between the gold film and the NS layer (hot spot B) in addition to hot spot A. This interlayer electric field is formed by the light-driven oscillation of conduction electrons in the NS, which induces secondary oscillation of their image charges in the gold film. Therefore, this interlayer electric field is mainly z-polarized.[28,29] While the graphene sheet placed at the interlayer experiences this increased local field, its major Raman peaks are not greatly enhanced since their vibrations are in-plane. The graphene sheet in the NS-g-Film sample is not corrugated to the extent as in the g-NS sample since interaction with the flat film is stronger. For these reasons, the SERS enhancement in the NS-g-Film is only slightly larger than the g-Film and is much less than the g-NS.

In the NS-g-NS sample, the graphene sheet is positioned at the interlayer and experiences the enhanced local field from hot spot B. While the effect of this hot spot on the SERS is small because of the aforementioned polarization direction, parts of the graphene experience the high local field generated from hot spot A as the graphene sheet can be corrugated. Therefore, the SERS enhancement of the NS-g-NS is as high as the g-NS.

The high local electric field not only enhances the Raman signal, but also induces deformation of the graphene sheet and distortion of the Raman spectrum. This is significant in the 633 nm excitation of the g-NS, NS-g-Film, and NS-g-NS.

Conclusions

In this work, surface enhanced Raman scattering (SERS) was applied to 2-dimensional graphene sheets on various gold substrates. Observed Raman enhancements of 3 ~ 50 times can be explained with an electromagnetic mechanism rather than chemical mechanism. A model based on the local field distribution and orientation of the graphene sheet was proposed to explain the difference of the Raman enhancements in different structures of the gold substrates. In all the samples, the enhancements were not as great as in the case of molecular adsorbates as the graphene cannot be positioned at the intralayer hot spots of the local electric field. The graphene sheet is thought of being corrugated along the curvature of the substrate and thereby may approach closer to the hot spots in the case of nanosphere sub-

strates. When the graphene is sandwiched between two gold layers, the Raman signal is enhanced only moderately as the interlayer local electric field is polarized incorrectly.

Some Raman spectra are distorted with the appearance of unidentifiable peaks as well as enhancement of broadened D peaks. As the degree and condition for the spectrum distortions are parallel with those of Raman enhancements, the high local field seems to have caused a laser-induced graphene deformation.

Supporting Information. The followings are available on-line as supplementary materials; AFM, SEM, and optical microscope images of samples; laser-induced distortion of spectra; a local field distribution calculated using FDTD method.

References

1. Novoselov, K. S.; Geim, A. K.; Morozov, S. V.; Jiang, D.; Zhang, Y.; Dubonos, S. V.; Grigorieva, I. V.; Firsov, A. A. *Science* **2004**, *306*, 666.
2. Kim, K. S.; Zhao, Y.; Jang, H.; Lee, S. Y.; Kim, J. M.; Kim, K. S.; Ahn, J.-H.; Kim, P.; Choi, J.-Y.; Hong, B. H. *Nature* **2009**, *457*, 706.
3. Li, X.; Cai, W.; Ahn, J.; Kim, S.; Nah, J.; Yang, D.; Piner, R.; Velamakanni, A.; Jung, I.; Tutuc, E.; Banerjee, S. K.; Colombo, L.; Ruoff, R. S. *Science* **2009**, *324*, 1312.
4. Reina, A.; Jia, X.; Ho, J.; Nezich, D.; Son, H.; Bulovic, V.; Dresselhaus, M. S.; Kong, J. *Nano Lett.* **2009**, *9*, 30.
5. Wallace, P. R. *Phys. Rev.* **1947**, *71*, 622.
6. Neto, A. H. C.; Guinea, F.; Peres, N. M. R.; Novoselov, K. S.; Geim, A. K. *Rev. Mod. Phys.* **2009**, *81*, 109.
7. Tuinstra, F.; Koenig, J. L. *J. Chem. Phys.* **1970**, *53*, 1126.
8. Reich, S.; Thomsen, C. *Phil. Trans. R. Soc. Lond. A* **2004**, *362*, 2271.
9. Thomsen, C.; Reich, S. *Phys. Rev. Lett.* **2000**, *85*, 5214.
10. Saito, R.; Jorio, A.; Souza Filho, A. G.; Dresselhaus, G. ; Dresselhaus, M. S.; Pimenta, M. A. *Phys. Rev. Lett.* **2002**, *88*, 027401.
11. Casiraghi, C.; Hartschuh, A.; Qian, H.; Piscanec, S.; Georgi, C.; Fasoli, A.; Novoselov, K. S.; Basko, D. M.; Ferrai, A. C. *Nano Lett.* **2009**, *9*, 1433.
12. Park, J. S.; Reina, A.; Saito, R.; Kong, J.; Dresselhaus, G.; Dresselhaus, M. S. *Carbon* **2009**, *47*, 1303.
13. Ferrai, A. C.; Meyer, J. C.; Scardaci, V.; Casiraghi, C.; Lazzeri, M.; Mauri, F.; Piscanec, S.; Jiang, D.; Novoselov, K. S.; Roth, S.; Geim, A. K. *Phys. Rev. Lett.* **2006**, *97*, 187401.
14. Wang, Y. Y.; Ni, Z. H.; Yu, T.; Shen, Z. X.; Wang, H. M.; Wu, Y. H.; Chen, W.; Wee, A. T. S. *J. Phys. Chem. C* **2008**, *112*, 10637.
15. Ni, Z. H.; Chen, W.; Fan, X. F.; Kuo, J. L.; Yu, T.; Wee, A. T. S.; Shen, Z. X. *Phys. Rev. B* **2008**, *77*, 115416.
16. Calizo, I.; Bao, W.; Miao, F.; Lau, C. N.; Balandin, A. A. *Appl. Phys. Lett.* **2007**, *91*, 201904.
17. Calizo, I.; Ghosh, S.; Bao, W.; Miao, F.; Lau, C. N.; Balandin, A. A. *Sol. Stat. Comm.* **2009**, *149*, 1132.
18. Das, A.; Chakraborty, B.; Sood, A. K. *Bull. Mater. Sci.* **2008**, *31*, 579.
19. Goncalves, G.; Marques, P. A. A. P.; Granadeiro, C. M.; Nogueira, H. I. S.; Singh, M. K.; Grácio, J. *Chem. Mater.* **2009**, *21*, 4796.
20. Aroca, R. *Surface Enhanced Vibrational Spectroscopy*; John Wiley & Sons: 2006.

21. Yoon, J. K.; Kim, K.; Shin, K. S. *J. Phys. Chem. C* **2009**, *113*, 1769.
22. Park, W.-H.; Ahn, S.-H.; Kim, Z. H. *ChemPhysChem* **2008**, *9*, 2491.
23. Le, F.; Lwin, N. Z.; Steele, J. M.; Käll, M.; Hallas, N. J.; Nordlander, P. *Nano Lett.* **2005**, *5*, 2009.
24. Christ, A.; Zentgraf, T.; Tikhodeev, S. G.; Gippius, N. A.; Martin, O, J, F.; Kuhl, J.; Giessen, H. *Phys. Stat. Sol. (b)* **2006**, *243*, 2344.
25. Jung, H. Y.; Park, Y.-K.; Park, S.; Kim, S. K. *Anal. Chim. Act.* **2007**, *602*, 236.
26. Yun, S.; Park, Y.-K.; Park, S.; Kim, S. K. *Anal. Chem.* **2007**, *79*, 8584.
27. Yun, S.; Oh, M. K.; Kim, S. K.; Park, S. *J. Phys. Chem. C* **2009**, *113*, 13551.

28. Oh, M. K.; Yun, S.; Kim, S. K.; Park, S. *Anal. Chim. Act.* **2009**, *649*, 111.
29. Oh, M. K.; Kim, S. K.; Park, S.; Lim, S. *J. Compt. Theor. Nanosci.* **2010**, *7*, 1085.
30. Wang, Y. Y.; Ni, Z. H.; Shen, Z. X.; Wang, H. M.; Wu, Y. H. *Appl. Phys. Lett.* **2008**, *92*, 043121.
31. Gierz, I.; Riedl, C.; Starke, U.; Ast, C. R.; Kern, K. *Nano Lett.* **2008**, *8*, 4603.
32. Giovannetti, G.; Khomyakov, P. A.; Brocks, G.; Karpan, V. M.; Brink, J. van den.; Kelly, P. J. *Phys. Rev. Lett.* **2008**, *101*, 026803.
33. Chan, K. T.; Neaton, J. B.; Cohen, M. L. *Phys. Rev. B* **2008**, *77*, 235430.
34. Ishigami, M.; Chen, J. H.; Cullen, W. G.; Fuhrer, M. S.; Williams, E. D. *Nano Lett.* **2007**, *7*, 1643.